Foam drainage on thick porous substrate

Toby Armstrong, Hannah Smith, Omid Arjmandi-Tash, Jennifer Cook, Anna Trybala, Victor Starov

Department of Chemical Engineering, Loughborough University, Loughborough, Leics. LE11 3TU, UK

Corresponding author: a.trybala@lboro.ac.uk (Anna Trybala)

Abstract: The use of foam-based applications as a method of drug delivery represents a recent and promising area of research. The interaction of foam and porous substrates have been recently theoretically described using a mathematical model, which combines the equation of foam drainage with that of imbibition of liquid into the porous substrate. Below the drainage of foam placed on chalk experimentally investigated to verify the theory prediction. The surfactants sodium dodecyl sulfate (SDS) and Triton X-100 were used to form a foam. The initial liquid volume fractions of the foam were found to be ranging in between 14.12 and 16.46%. The porosity and permeability of the chalk substrate were experimentally obtained at 59.1% and $3.122 \cdot 10^{-11}$ m² respectively. The height of foam deposited onto the thick porous substrate (chalk) was 2.5 cm and 6 cm. The imbibition into the chalk, the height of foam, and the bubble size within the foam were monitored. The latter enabled the kinetics of the drainage/imbibition to be determined and compared with the predictions according to the theoretical model. The rate of decrease in foam height was initially high and decreased over time as predicted by the theoretical model. All the foam displayed an initial rapid imbibition through the porous substrate, which is again in the agreement with the theory predictions. It was found that solutions with lower surfactant concentrations could penetrate deeper into the chalk. The imbibition front was observed to be uniform: evenly distributed liquid throughout the cross-section of the porous substrate.

1. Introduction

Foams are multiphase mixtures, colloidal systems comprised of a gas in the dispersed phase and a liquid in the continuous phase (Malysa, 1992). Foams are used in a variety of industries, with applications in medicine, petroleum, foods, pharmaceuticals and cosmetics (Exerowa and Kruglyakov, 1998; Schramm, 2000; Koehler et al., 2000; Bureiko et al., 2015). Most recently, foams have been introduced in pharmacy as a method of drug delivery. It was found in dermatology that patients preferred the application of medications as foams over traditional applications as creams, ointments and gels (Arzhavitina and Steckel, 2010). The comparatively lower density of foams gives a feeling of a gentler application (Purdon et al., 2003), and the speed at which the foam is absorbed proves effective on areas of skin with hair growth (Del Rosso, 2002). The high consumer acceptance of foams is conducive to their increased use in pharmaceutical and cosmetic industries, making foams an area of research which is currently attracting interest.

Pure liquids cannot make a foam without the addition of a foaming agent (Bikerman, 1953) (surfactant, surfactant-polymer mixture). Foaming occurs when the resultant solution undergoes either a mechanical processing (such as shaking or whipping) or the liquid phase is supersaturated with gas (Arzhavitina and Steckel, 2010). Foam structure is characterised by the gas volume fraction and the bubble size. For smaller bubble sizes and lower volume fractions, the bubbles may be assumed to be spherical in shape and equal in size (Arzhavitina and Steckel, 2010). At higher volume fractions and larger bubble sizes, the bubbles deform, producing polyhedral bubble shapes (Princen

and Kiss, 1989). The spaces between the gas bubbles are divided into three categories: (a) lamellae, the film surface between adjacent bubbles, (b) Plateau borders, channels where three films meet, and (c) nodes, the junctions where four channels meet (Koehler et al., 2000). The flow of liquid through these spaces is referred to as foam drainage.

Free foam drainage begins as soon as the foam is formed (Exerowa and Kruglyakov, 1998) and is governed by a competition between two forces: gravity and capillarity. The lower density of the air bubbles causes them to rise while gravity causes liquid to drain downwards through the bubbles (Arzhavitina and Steckel, 2010). Drainage eventually results in a varying liquid content over the foam height, from the highest at the bottom and the lowest at the top. Although foam drainage is well-researched, an investigation into foam drainage in contact with a porous substrate has been only recent undertaken (Bureiko, 2015; Arjmandi-Tash, 2015). When a foam is placed onto a porous substrate, the liquid is drained through the porous substrate by the action of gravity and suction into the porous substrate; this results in both faster drainage and a drier resulting foam (Arjmandi-Tash, 2015).

Foam drainage on a porous substrate is important in the pharmaceutical and cosmetic industries, where the foam is used to apply the intended product onto skin or hair, which is a porous material. Research into the kinetics of foam drainage placed on a porous substrate are of particular interest when considering the use of foam in drug application because the speed and manner in which liquid imbibition occurs into the porous substrate have implications for the delivery of active substances in the foaming liquid onto skin and hair. A mathematical model for foam drainage placed on a porous substrate was earlier presented (Bureiko, 2015) and investigated using computer simulations (Arjmandi-Tash, 2015). It was found that foam drainage on a porous substrate occurred in 3 different regimes: (a) rapid imbibition, (b) intermediate imbibition, and (c) slow imbibition, depending on the initial liquid volume fraction of the foam and 3 dimensionless numbers (Arjmandi-Tash, 2015).

The presented work aims to test the model of foam drainage placed on a thick porous substrate, using chalk as a model porous substrate. The imbibition of liquid from the foam into the chalk is investigated experimentally, using foam made of Newtonian liquids (aqueous surfactants solutions). The effect of the concentration of surfactant used to generate foam solutions and imbibition process is presented.

2. Materials and methods

2.1 Foam

Sodium Dodecyl Sulfate (SDS) purchased from ACROS Organics, and Triton X-100, purchased from SIGMA Life Science were used with distilled water to prepare solutions for foam generation. Solutions were made at varying concentrations shown in Table 1.

Table 1. Surfactants concentrations used for foam generations

Concentration (CMC)	Mass (g/dm^3)
SDS (CMC = 8.2 mM)	
2	4.2780
4	9.4560
5	11.8200
Triton X-100 (CMC = 0.24 mM)	
20	3.6232
50	9.0580

The initial liquid volume fraction of each foam was measured by dividing the weight of the liquid in a known volume of foam by the density of the solution. The densities of all solutions were assumed equal to that of water, due to the low concentrations of surfactants. Measurements were repeated 3 times to give an average value and the standard deviation.

2.2 Porous substrate

Cylindrical samples of chalk purchased from Poundland were used as model thick porous substrates. The chalk was cut and sanded to 4 cm in length. The diameters varied from 2.46 - 2.52 cm. Each piece was glued to the bottom of a glass tube (as shown in Figure 1) with an outer diameter of 2.54 cm using Wilkinson's own brand All Purpose Adhesive, and left for a minimum of 30 minutes to ensure a strong and water tight seal between the outer diameter of the tube and the chalk face.

The porosity of the chalk was calculated by measuring the penetration depth and diameter of a known volume of water when it had been deposited on the chalk. This was achieved experimentally using the set up shown in Fig. 1 using camera 1 only for this measurement. A 5 cm³ of distilled water was deposited within the tube with time zero occurring when the water made contact with the chalk face. Image analysis was then used in order to show the rate of imbibition through the chalk. The measurement was ended when all the water was absorbed by the chalk. This procedure was repeated for 5 pieces of chalk to give an average porosity value and the standard deviation.

$$Porosity\ (\epsilon) = \frac{Pore\ volume\ (V_p)}{Total\ wetted\ volume\ (V_t)}. \tag{1}$$

Equation 1 was used to calculate the porosity of the chalk. The pore volume (V_p) was equated to the known volume of distilled water, and the tapered cylindrical shape of the porous substrate was taken into account when calculating the total wetted volume (V_t). Image analysis was used in order to precisely measure the chalk-water interface diameter and the depth of penetration through the chalk with respect to time. When all of the water had been absorbed, the total wetted volume (V_t) was measured and a final porosity was calculated.

The Kozeny-Carman (Carman, 1939) model was used to calculate the permeability in the chalk. The permeability (k) of the chalk was calculated by monitoring the imbibition through the chalk (h) with respect to time according to the experiment described above. Darcy's law (H.P.G. Darcy, 1856)

$$Q = \frac{k}{\mu}\frac{\Delta P}{\Delta h}A \tag{2}$$

is initially used in order to describe the kinetics of fluid flow through a porous medium in terms of a driving force and the permeability. The flowrate Q using the porosity and the rate of imbibition with respect to time is:

$$Q = \epsilon\frac{dh}{dt}. \tag{3}$$

The Young-Laplace equation was used in order to describe the capillary pressure difference across the capillary meniscus interface between the liquid inside the capillary and air:

$$\Delta P = \frac{2\gamma}{R_{ps}}, \tag{4}$$

where surface tension (γ) and the average pore size (R_{ps}) within the porous substrate, respectively. Permeability can be calculated combining Equations 2, 3 and 4 as follows:

$$h^2 = \frac{4k\gamma}{\epsilon\mu R_{ps}}t. \tag{5}$$

By monitoring h with respect to time and plotting h^2 vs. t, the slope of the regression line was used in order to determine the permeability of the chalk.

2.3. Experimental procedure

Two Pike Allied Vision Technologies cameras were used to monitor the foam height, imbibition through substrate and bubble size (Fig. 1); camera 1 using a Sony TV Lens 1:1.8 16 mm (wide angle) focussed on the whole glass column and chalk, and camera 2 using a Cosmicar TV Zoom Lens 12.5~75 mm 1:1.8 focussed on a small section of the foam to monitor bubble size. The cameras were set to take 7.5 frames per second. A glass column was used to hold the foam, and it was clamped vertically using a ruler (as a scale) next to it for reference.
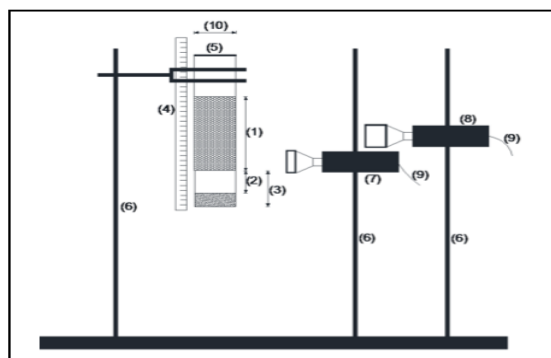
Fig. 1. The experimental set-up; (1) foam in glass tube, (2) imbibition trough porous substrate (chalk), (3) chalk, (4) scale, (5) column seal, (6) stands, (7) camera 1, (8) camera 2, (9) interface to PC, (10) column diameter

The foam was produced using a Clairol Nice'n'Easy foaming bottle, which had a tube attached to the nozzle to allow an accurate and even application of foam into the tube. The foam was injected into the column at heights of approximately 6 cm or 2.5 cm. After that, the column was covered with a parafilm seal to prevent evaporation. The experiments were run for 10 minutes for SDS, and between 4-6 minutes for Triton X-100 depending on the stability of the foam.

Images at 0, 0.5, 1, 1.5, 2, 3, 4, 5, 6, 7 and 8 minutes for the foam height and bubble size were used. The imbibition into the chalk was analysed every 50 frames, which is equal to every 6.667 seconds. Due to the big diameter of the chalk measurements for imbibition were taken at the left-hand side, middle and right-hand side of the chalk, and then averaged to find a mean. 6 runs were completed for each foaming solution (Table 1) at both 2.5 cm and 6 cm initial heights of the foam. Images were analyzed using ImageJ image analysis software (Fig. 2).
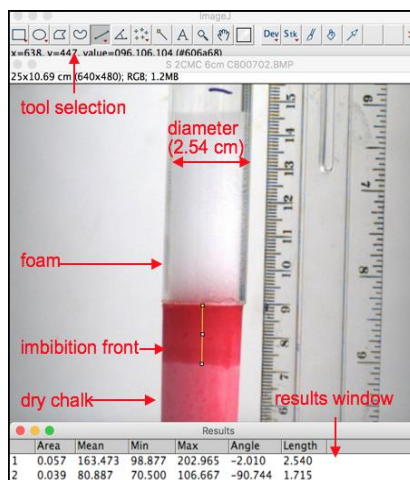

Fig. 2. Measurement of the imbibition front (screenshot from ImageJ software); the yellow line is equal to 1.715 cm

3. Results and discussion

3.1. Foam development

Liquid drainage in foam forces gas upwards. This causes degradation of the foam through film rupture; therefore, as the foam bubbles rupture the foam height is expected to decrease. The initial height of the foam for each experiment was set either 2.5 cm or 6 cm; however, the actual average initial heights were 2.654±0.148 cm and 6.001±0.116 cm. The initial foam generation occurred rapidly, therefore the initial heights of the 2.5 cm foam column showed greater variance than those of the 6 cm column. The foam height was measured every 30 seconds for the first 2 minutes, and every minute after that until the end of the experiment. The experiment ended when the foam height became so small that it was difficult to detect by the cameras, or the foam structure began to collapse. The

remaining liquid inside the foam at this moment was so low that liquid drainage could be negligible. Experimental results on measurements of the foam height are presented in Fig. 3.
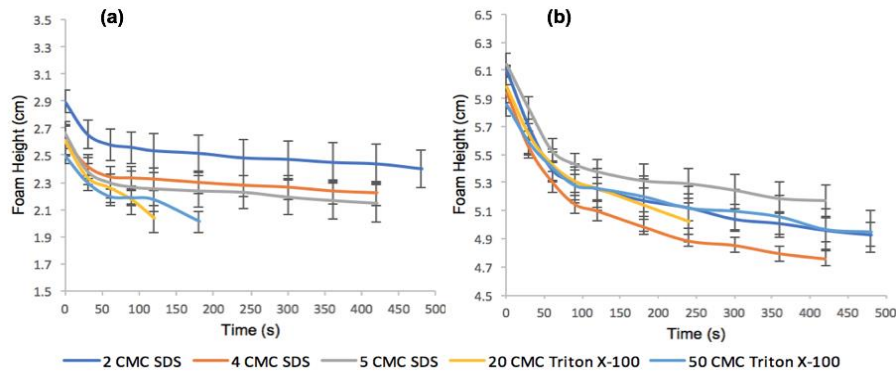

Fig. 3. Time evolution of foam height for initial foam heights (a) 2.5 cm and (b) 6 cm

It was predicted earlier that foam drainage placed on a porous substrate occurs initially both at the top of the foam and the foam/substrate interface only (Bureiko, 2015), with an initial rapid decrease in liquid volume fraction at the interface (Arjmandi-Tash, 2015). After that (according to the theory predictions), a slower process of the drainage from the main body of the foam start, which results in a slower foam height decrease. This conclusion is supported by our data presented in Figure 3. According to experimental results presented in Fig. 3, the whole process can be subdivided roughly into two stages: (*i*) a relatively fast decrease of the foam height, which is followed by the second stage (*ii*) of a slower decrease of the foam height. Presence of these two stages for the 2.5 cm foam the initial fast decrease was approximately 0.4 cm in the first 30 - 45 seconds (Fig. 3a). Comparing this with the 6 cm foam columns, the initial rapid decrease period was longer (Fig. 3b). The rate of height decrease slowed over time in all cases after the initial rapid period.

The higher stability of SDS is consistent with a recent study (Osei-Bonsu, 2015) which determined that the half-decay time of SDS was larger than that of Triton X-100. This is due to the non-ionic charge on Triton X-100, compared to the anionic charge on SDS; ionic surfactants are known to form more stable foams due to strengthening effects of charge interactions at the film interface, which do not occur in non-ionic surfactants (Osei-Bonsu, 2015). The CMC value of foam solution seemed to have no bearing on either the speed or the amount of decrease in foam height. This is consistent with an earlier study on surfactant foam stability (Rothmel, 1998) which determined that foam stability is independent of the concentration.
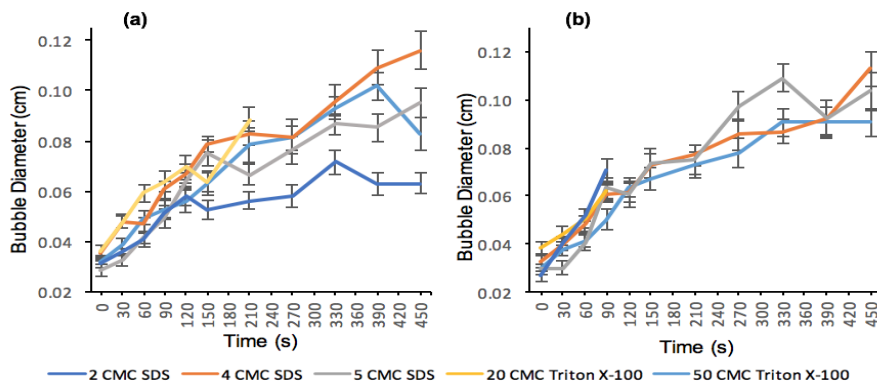

Fig. 4. Time evolution of bubble size for initial foam heights (a) 2.5 cm and (b) 6 cm

The degradation of the foam can also be assessed through analysis of the bubble size. As foam drainage occurs gas is forced upwards until the bubbles collapse. This happens either through rupture of thin films between bubbles or through Ostwald ripening (absorption of smaller bubbles by larger ones) (Eren, 2004). Therefore, it was expected to see an increase in bubble size as time progressed. The

bubble shape was approximated to be spherical when assessing the bubble size. Results are shown in Fig. 4.

The initial bubble diameters of all five foams were relatively similar, ranging from 0.0265±0.011 cm to 0.0384±0.015 cm for 2.5 cm at initial heights (Fig. 4a), and 0.024±0.012 cm to 0.031±0.014 cm for 6 cm at initial foam heights (Fig. 4b). A recent study (Osei-Bonsu, 2015) also found that SDS and Triton X-100 foams displayed initially similar bubble size distributions.

Figure 4 confirms the predicted increase of bubble diameter over time for all foaming solutions. This is a result of a decrease in the liquid volume fraction inside the foam, which is clearly visible as the foam degrades; the resultant foam becomes noticeably transparent as the liquid drains from the lamellae. Figure 5 gives a visual example of the bubble size at the beginning (Fig. 5a) and end (Fig. 5b) of an experiment. Here it is clear that the bubble size has increased and the lamellae have thinned.
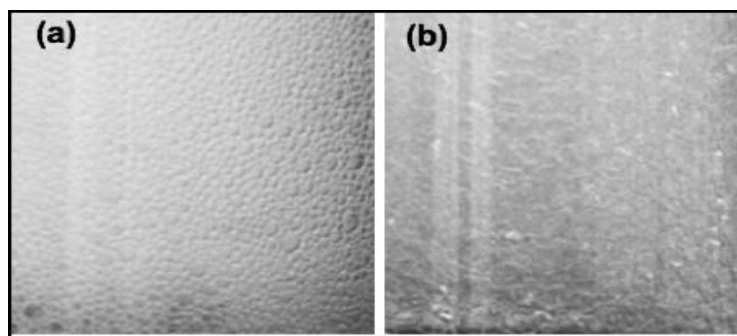

Fig. 5. Foam height at (a) the beginning and (b) the end of the experiment

In some cases, it was observed that a large air bubble formed at the the foam/chalk interface (the bottom of the column). This eventually caused the foam to detach from the porous substrate completely (Fig. 6). The detachment was more commonly seen in the 6 cm foam columns than the 2.5 cm columns; exceptions to this were the experiments on SDS 5 CMC, where detachment was seen more regularly in the 2.5 cm columns, and Triton X-100 20 CMC, where detachment was seen less frequently for both column heights.

It was assumed (Bureiko, 2015; Arjmandi-Tash, 2015) that there is a critical volume fraction of the liquid fraction in the foam when the thin films between bubbles start to rupture. As it was mentioned above the liquid fraction at the foam/porous substrate interface can only decrease. In some cases, this liquid fraction can reach the critical values, after that the bubbles at the bottom start bursting and forming the big bubble, which eventually detaches the foam from the porous substrate (Fig. 7).
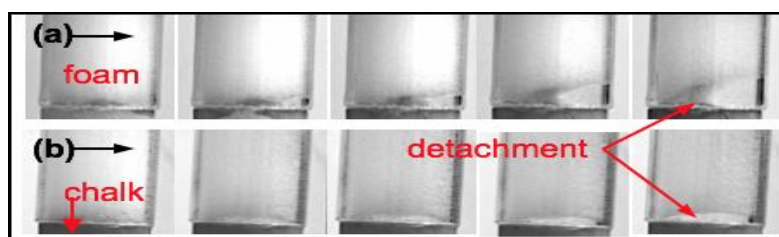

Fig. 6. Development of foam detachment resulting from an air bubble formation at the bottom

3.2 Imbibition into substrate

For foam drainage placed on a porous substrate, the kinetics of the process were expected to follow one of three regimes - either slow, intermediate, or rapid imbibition (Bureiko, 2015; Arjmandi-Tash, 2015). Theoretically, the regime is dependent on the ratio of the capillary pressure in the porous substrate to that in foam, Bond number, the porosity of the porous substrate and the initial liquid volume fraction (Arjmandi-Tash, 2015).

An average porosity ($\in$) of chalk was found to be very high compared to the literature values for natural chalk (5 - 40 %) this is possibly due to dissolution (secondary porosity), which is known to

occur particularly in carbonates (Glover, 2008). The chalk may also have been altered during processing; for example, it could have been made synthetically less dense to make it safer and easier to use for children. The average permeability was calculated as described above (3.122×10^{-11} m^{-2}).

Table 2 gives the average initial liquid volume fractions for each of the individual foam solutions. These values are reasonably high; however, since the porosity value is considerably larger than the liquid volume fraction of all the foam solutions, the model predicts that the process will follow the rapid imbibition regime (Arjmandi-Tash, 2015).

Table 2. Initial liquid volume fractions for foam solutions

Concentration (CMC)	Average Initial Liquid Volume Fraction (%)	Standard Deviation (%)
SDS		
2	16.46	0.67
4	14.87	0.41
5	14.64	0.92
Triton X-100		
20	14.12	0.47
50	16.46	0.08

Both imbibitions into the substrate and the conditions at the foam/chalk interface were monitored during foam drainage on a thick porous substrate (chalk). It was expected that a free liquid layer would be formed at the interface if the imbibition into the porous substrate was slower than the drainage of the foam (Arjmandi-Tash, 2015). However, this was not observed for any experiment, indicating that the imbibition into the chalk occurred faster than the drainage of the foam. This suggests that the drainage/imbibition followed the rapid regime, as predicted (Arjmandi-Tash, 2015).

The imbibition into the substrate was analysed every 50 frames (equal to every 6.667 seconds) until the foam had sufficiently degraded. From the analysis of the foam development (see Figure 3), it was seen that this point was reached after 7 - 8 minutes for the SDS foam solutions. The Triton X-100 foams were less stable than the SDS foam, and therefore the foam had often degraded earlier before 5 minutes.
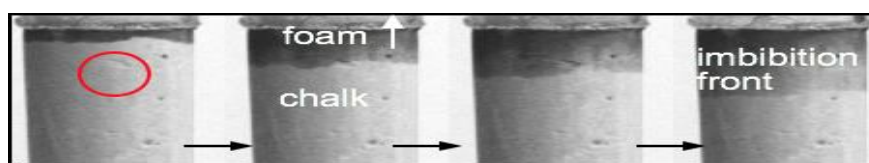

Fig. 7. Effect on an imperfection in chalk (circled) on the uniformity of imbibition

Measurements were taken from the base of the foam column to the edge of the visible penetration front, referred to as the imbibition front (Figs. 2 and 7). The chalk often had imperfections which affected the precise location of the imbibition front; an example is shown in Fig. 7. Although non-uniform imbibition is demonstrated in the region of the imperfection, eventually the imbibition regains uniformity. Anomalous results due to these imperfections were avoided by taking multiple measurements across the width of the chalk; this showed that imbibition continued in general, even if an imperfection has slowed the imbibition front in one location. The results are shown in Fig. 8. The similarity between the standard error for all points made it possible to omit some error bars in order to make the graphs in Fig. 8 (a and b) easier to read; error bars have been included for every three data points.

All solutions displayed an initial period of rapid imbibition. This supports the theory that the drainage/imbibition process begins with an initial rapid decrease in liquid volume fraction at the foam/substrate interface (Arjmandi-Tash, 2015). The liquid leaving the foam penetrates the substrate, as expected, giving the initial rapid imbibition shown in Fig. 8.
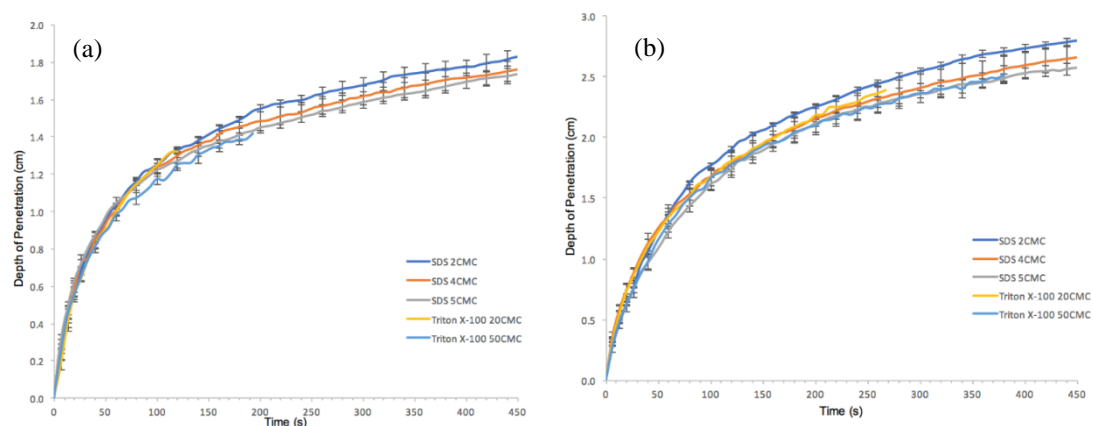
Fig 8a. Time evolution of the depth of liquid penetration into the porous substrate for foams made of SDS and Triton X-100 for (a) 2.5 cm initial foam height, (b) 6 cm initial foam height

The rate of the initial imbibition is the same for both 2.5 cm and 6 cm initial foam heights, however, period of rapid imbibition lasts longer for the 6 cm foam column as expected. The rate of penetration then decreased gradually over time until the end of the experiment; it is obvious that the depth of penetration would reach eventually plateau if the experiment was continued further. The average final depth of penetration into chalk in compared in Table 3. The final depth of penetration is determined purely by the mass balance. The difference is explained by the different initial volume fraction of water in the foam.

Table 3. Average final depth of penetration into chalk

Initial foam height	Concentration (CMC)	Final depth of penetration (cm)	Standard deviation (%)
	SDS		
	2	1.882	0.104
2.5 cm	4	1.767	0.052
	5	1.741	0.089
	Triton X-100		
	20	1.324	0.024
	50	1.422	0.052
	SDS		
	2	2.803	0.052
6 cm	4	2.667	0.159
	5	2.573	0.093
	Triton X-100		
	20	2.387	0.111
	50	2.518	0.141

The imbibition through the cross-section of the chalk was consistently uniform, as shown in Fig. 9. The horizontal striped patterns inside the chalk are a result of the handsaw used to cut the chalk in half lengthways to view the cross-section. The colour of the chalk had no effect on the kinetics of imbibition; the only difference between the colours was that imbibition was more visible for darker colours of chalk.
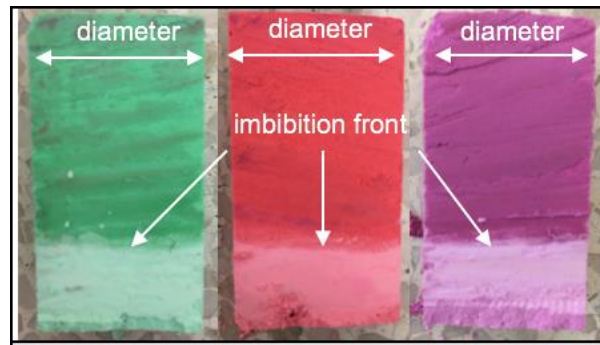
Fig. 9. Cross-sections of different coloured chalk showing the uniformity of imbibition

4. Conclusions

The proposed earlier model for foam drainage placed on a porous substrate was tested using surfactant foam on a thick porous substrate (chalk). The comparison showed a good agreement between the theory predictions and the observed experimental measurements. The foam drainage placed on a thick porous substrate was experimentally investigated. Chalk was used as a porous substrate to avoid possible influence of swelling of the porous substrate. Time evolution of the foam heights averages bubble size and the depth of penetration into the porous substrate was monitored. It was shown that the bubble size for all foams investigated increased over time, according to a decrease in liquid volume fraction as drainage/penetration proceeds. It was found that the height of the foam column initially decreased rapidly, and then the rate decreased over time. This behaviour supports the predicted earlier initial rapid decrease in liquid volume fraction at the foam/chalk interface. The imbibition was consistently uniform, and no free liquid layer formation was detected in accordance with the theory predictions. The examined parameters were shown to support the proposed model, with the process following the rapid imbibition regime. The detachment of the foam column - behaviour has been observed and explained.

Nomenclature

A — area, m^2
CMC — critical micelle concentration
h — the depth of imbibition into the substrate, m
k — permeability, m^{-2}
P — capillary pressure, Pa
Q — flowrate, m^2 s^{-1}
R_{ps} — pore size in the substrate, m
SDS — Sodium Dodecyl Sulfate
t — time, s
V_p — pore volume, m^3
V_t — total wetted volume, m^3
ϵ — porosity, %
γ — surface tension, N m^{-1}
μ — viscosity, Pa s

References

ARJMANDI-TASH O., KOVALCHUK N., TRYBALA A. and STAROV V., 2015. *Foam drainage placed on a porous substrate*. Soft Matter, 11, 3643-3652.

ARZHAVITINA A. and STECKEL H., 2010. *Foams for pharmaceutical and cosmetic application*. Int. J. Pharma., 394, 1-17.

BIKERMAN J.J., 1953, *Foams,* pp.99, Springer-Verlag, California.

BUREIKO A., ARJMANDI-TASH O., KOVALCHUK N., TRYBALA A. and STAROV V., 2015. *Interaction of foam with a porous medium: Theory and calculations.* Eur. Phys. J. Special Topics, 224, 459-471

BUREIKO A., TRYBALA A., KOVALCHUK N., and STAROV V., 2015. *Current applications of foams formed from mixed surfactant-polymer solutions.* Adv. Colloid Interf. Sci., 222, 670-677

DEL ROSSO J.Q., 2002. *Using a foam vehicle for dermatologic applications.* [ONLINE] Available at: http://www.the-dermatologist.com/article/625 [Accessed 23/02/17].

EREN T., 2004. *Foam characterization: Bubble size and texture effects.* MSci thesis, Middle East Technical University, Turkey

EXEROWA D. and KRUGLYAKOV P.M., 1998. *Foam and Foam Films; Theory, Experiment, Application.* pp.381 & 738, Elsevier, Amsterdam

GLOVER P., 2008. *Petrophysics.* [ONLINE] Available at: http://homepages.see.leeds.ac. uk/~earpwjg/PG_EN/CD%20Contents/GGL-66565%20Petrophysics%20English/Chapter%202.PDF [Accessed 13/03/17].

H.P.G. Darcy, D´etermination des lois d´´ecoulement de l´eau `a travers le sable (1856).

KOEHLER S.A., HILGENFELDT S. and STONE H.A., 2000. Generalized View of Foam Drainage: Experiment and Theory, *Langmuir*, 16, 6327-6341

MALYSA K., 1992. *Wet foams: formation, properties and mechanism of stability.* Adv. Colloid Interf. Sci., 40, 37-83

OSEI-BONSU K., SHOKRI N. and GRASSIA P., 2015. *Foam stability in the presence and absence of hydrocarbons: from bubble- to bulk-scale.* Colloids and Surfaces A: Physiochem. Eng Aspects, 481, 514-526

P. CARMAN, 1939. *Permeability of saturated sands, soils and clays.* J. Agricult. Sci. 29, 262-273.

PRINCEN H.M. and KISS A.D., 1989. *Rheology of foams and highly concentrated emulsions.* J. Colloid Interf. Sci., 128, 176-187

PURDON C.H., HAIGH J.M., SURBER C. and SMITH E.W., 2003. *Foam drug delivery in dermatology.* Am. J. Drug Del., 1, 71-75

ROTHMEL R.K., PETERS R.W., MARTIN E.S. and DEFLAUN M.F., 1998. *Surfactant foam/bioaugmentation technology for in situ treatment of TCE-DNAPLs.* Envrion. Sci. Tech., 32, 1667-1675

SCHRAMM L., 2000. *Surfactants: Fundamentals and Applications in the Petroleum Industry.* Cambridge University Press, Cambridge, pp.79.